

RESEARCH

Open Access



Integrative analysis of transcriptome and metabolism reveals functional roles of redox homeostasis in low light and salt combined stress in *Leymus chinensis*

Jikai Li^{1,2*}, Suyang Fang², Hailing Zhang¹, Zubair Iqbal², Chen Shang¹, Weibo Han¹, Kai Huang², Xiangshen Meng², Muyuan Dai², Zhiheng Lu², Bingnan Guo² and Mingnan Qu^{2*}

Abstract

Salt stress is one of the major limiting factors of *Leymus chinensis* (named sheepgrass) growth, which accelerates inhibitive effects that are particularly concomitant with low light regimes (LL-Salt). However, little is known about physiological and molecular mechanisms under such LL-Salt in sheepgrass. This study aims to uncover the key reprogrammed metabolic pathways induced by LL-Salt through an integrated analysis of transcriptome and metabolism. Results suggested that the growth of sheepgrass seedlings was dramatically inhibited with a ranging of 8 to 20% reduction in F_v/F_m in LL-Salt combined treatments. Catalase activities were increased by 40% in LL but significantly decreased in salt stress, ranging from 15 to 46%. Both transcriptome and metabolism analysis reveal that carbon metabolism pathways were significantly enriched in the differentially expressed genes with downregulation by both LL and salt stress treatment. Metabolites involved in the photorespiration pathway, including serine and glycolate, were downregulated in LL while upregulated in salt stress treatment, with the same pattern of expression levels of a photorespiration regulatory gene, glycolate oxidase. Collectively, we found that several antioxidant redox pathways, including photorespiration, GSG/GSSH redox, and ABA signaling, participated in response to LL and salt combined events and highlighted the roles of cellular redox homeostasis in LL-Salt response in sheepgrass.

Keywords Sheepgrass, Transcriptome, Photorespiration, ROS, Carbon metabolism, Antioxidant, TCA

*Correspondence:

Jikai Li
ljk8699466@163.com
Mingnan Qu
qmn@yzu.edu.cn

¹Institute of Grass Research, Heilongjiang Academy of Agricultural Sciences, Harbin 150086, China

²Jiangsu Key Laboratory of Crop Genomics and Molecular Breeding, College of Agriculture, Yangzhou University, Yangzhou 225009, China



© The Author(s) 2025. **Open Access** This article is licensed under a Creative Commons Attribution-NonCommercial-NoDerivatives 4.0 International License, which permits any non-commercial use, sharing, distribution and reproduction in any medium or format, as long as you give appropriate credit to the original author(s) and the source, provide a link to the Creative Commons licence, and indicate if you modified the licensed material. You do not have permission under this licence to share adapted material derived from this article or parts of it. The images or other third party material in this article are included in the article's Creative Commons licence, unless indicated otherwise in a credit line to the material. If material is not included in the article's Creative Commons licence and your intended use is not permitted by statutory regulation or exceeds the permitted use, you will need to obtain permission directly from the copyright holder. To view a copy of this licence, visit <http://creativecommons.org/licenses/by-nc-nd/4.0/>.

Introduction

Plants are constantly exposed to shade conditions due to many natural factors, such as high planting density, cloudy weather, smog, and self-shading. The agricultural importance of long-term shade is due to its deteriorative effect on crop yield [1]. *Leymus chinensis* is known as sheepgrass. It is a perennial plant from the Gramineae family [2]. Due to its high productivity and protein content, this species is increasingly recognized as a vital gramineous forage in Northern China and the Mongolian plateau, becoming a potential crop for grassland construction or renovation [3]. However, it was constantly exposed to highly salt soil conditions due to growth environments. Following the increasing demands of growing sheepgrass, high-density planting directly resulted in low light (LL) conditions. Therefore, LL becomes a non-negligible factor in reducing production, especially under LL concomitant with high salt conditions (LL-Salt). However, studies on physiological and molecular regulation in response to such LL-Salt combined events were less reported.

Generally, salt stress impairs plant growth through physiological aspects with two mechanisms: (1) enhanced osmotic stress (early response), the plant is unable to absorb water; (2) enhanced ion toxicity (secondary response), a secondary consequence of the effects caused by sodium ions on the functions of the cell, such as nutrient uptake, enzyme activity, photosynthesis, and metabolism [4]. Plants have adapted through various mechanisms to counteract the adverse effects of salt stress, such as inhibiting ROS production, enhancing antioxidant enzyme activities, accelerating carbon assimilation metabolism, controlling photorespiration, and mediating GSG/GSSH redox system and plant hormones [5]. Many master genes and biological pathways are involved in these responses to salt stress [6]. The Salt Overly Sensitive (SOS) pathway is a major plant signaling pathway that protects plants against salt stress [7, 8]. The SOS2-SOS3 kinase complex then interacts with and activates SOS1 to expel Na^+ out of the cell, prevent Na^+ accumulation, and promote salt tolerance. Besides the core SOS constituents, several new key regulators that fine-tune the SOS pathway, including Brassinosteroid Insensitive 2 (BIN2), GIGANTEA (GI), VPS23A, a component of the Endosomal Sorting Complex (ESCRT), and AtNN4, a calcium channel [9, 10].

Plants respond to light in numerous ways, from molecular-level changes to morphological changes [11–13]. In general, plants detect light regimes by sensing the low-red (R) to far-red (FR) ratio, which enhances phototropism controlled by the phototropin blue light receptors. Under such a light regime, the phytochrome B (phyB) is inactivated, leading to the activation of PHYTOCHROME INTERACTING FACTOR4 (PIF4), PIF5, and

PIF7 and triggering several physiological responses [14]. However, the most significant stresses experienced by plants are due to constant changes in light or exposure to extremely low or high light intensity levels in addition to salt stress [15]. Overstimulation of chloroplasts through chemical reactions initiates free radicals that react rapidly with oxygen to form reactive oxygen species (ROS), causing damage to cellular membranes, proteins, and other membrane-related components such as chlorophyll. However, how plants' morphological, physiological, and molecular regulator characteristics respond to low light intensities and salinity combined stress conditions remains unclear.

In this study, we performed a combined analysis of transcriptome and metabolism to uncover the key molecular regulators or metabolic pathways underlying the response of sheepgrass to LL-Salt combined stress. Six combinations of light (moderate light and low light) and salt stress (0mM, 50mM, and 200mM NaCl) were performed in sheepgrass seedlings. We systematically investigated the morphological and physiological traits in sheepgrass within 20 days of LL-Salt. Based on transcriptome analysis, GO and KEGG analysis suggested that many overlapped biological pathways were significantly enriched in light and salt response, but some have different regulatory patterns. In addition, metabolism analysis suggested a robust list of several overlapped metabolites that could be involved in the LL and salt stress response. Finally, we summarized the key metabolic pathways that co-respond to LL and salt stress and highlighted the vital role of redox homeostasis in response to both LL and salt stress in sheepgrass. This study may provide insight into how plants mediate cellular redox homeostasis to maintain growth development in such LL-Salt combined events in sheepgrass, which helps to guide precise molecular assistant selection in sheepgrass.

Materials and methods

Plant materials and LL-Salt treatments

Seeds of *L. chinensis* (SG045) were collected by Prof. Wei Li (Institute of Grass Research, Heilongjiang Academy of Agricultural Sciences) permitted by the Institute of Grass Research. The seeds were treated with 5% sodium hypochlorite for 5 min and washed 4 times in sterile distilled water for 12 h at room temperature, then transferred to moist filter paper for germination at room temperature 22–25 °C for 24 h. The seeds with uniform germination were selected and grown on plastic pots (a single plant was grown in one pot) in Hoagland solution, which was changed two days at an interval. Three-week-old seedlings were exposed to six combinations of light and salt treatments, i.e., ML_0, ML_50, ML_200, LL_0, LL_50, and LL_200 for 20 days, while ML_0 was used as control. Three salinity concentrations were applied

among the combinations, including 0 mM, 50 mM, and 200 mM NaCl. At the same time, two light treatments were also conducted, including moderate light (ML, 500 $\mu\text{mol m}^{-2}\text{s}^{-1}$ PPF) and low light (LL, 50 $\mu\text{mol m}^{-2}\text{s}^{-1}$ PPF). Five biological replicates were performed for each treatment.

Measuring physiological parameters

Soluble sugar and sucrose amounts were determined following the previous studies [16]. The standard method for proline was detected using the proline–ninhydrin reaction [17]. Three kits, including Catalog no.XG6, Catalog no. FY3 and Catalog no. EY2 was used to determine the activities of catalase (CAT), malondialdehyde (MDA), and peroxidase (POD), respectively, from Suzhou Keming Science and Technology Co, Ltd, China. In contrast, the activities of superoxide dismutase (SOD) were measured using a kit (Catalog no. A001-3) from the Nanjing Jiancheng Bioengineering Institute of Jiangsu Province, China. To minimize the experimental variability, three biological replicates were performed.

Maximal quantum yield

Maximal quantum yield (F_v/F_m) values were measured to estimate the photosynthetic capacity of sheepgrass caused by LL-Salt. F_v/F_m was measured using a Multi-Function Plant Efficiency Analyzer chlorophyll fluorometer (Hansatech) following [18]. F_m is the maximum chlorophyll fluorescence; F_0 is the minimum chlorophyll fluorescence, and $F_v = F_m \times 2 \times F_0$ [19].

Transcriptome analysis

Samples of leaves were collected from sheepgrass grown either under low light or two salt stresses. Total RNA was isolated using a TRIzol reagent (Invitrogen, Carlsbad, CA). The degradation and contamination of RNA were analyzed using 1% agarose gel electrophoresis, whereas purity was checked using the nano-photometer spectrophotometer (IMPLEN, CA, USA). The RNA's integrity was checked by applying the RNA Nano 6000 Assay Kit in combination with the Agilent Bioanalyzer 2100 system (Agilent Technologies, CA, USA). Each sample received 1.5 μg of RNA for the preparation of RNA samples. The preparation of sequencing libraries was done using the NEB Next Ultra RNA Library Prep Kit, which is suited for Illumina (NEB, USA) [20]. Libraries were post-cluster generation sequenced on an Illumina HiSeq 4000 platform, which produced paired-end reads of 150 bp and assessed the quality of RNA-seq data using software such as FastQC.

After the index of the genome was produced, the clean RNA-seq reads were mapped using STAR [21], which included ‘—quantMode GeneCounts’ to count the reads toward each gene. Next, genes and isoforms were

quantified using cufflinks version 2.2.1. Transcript levels for six light and salt combinations in sheepgrass leaves were determined by a differentially expressed genes (DEGs) analysis using Fragments Per Kilobase of transcript per Million mapped reads (FPKM). DEGs were identified with the help of the R package ‘DESeq2’ [22], which used count reads retrieved from STAR [21] for this study, and only genes with an adjusted *P*-value of less than 0.05 qualified as DEGs. This reduced transcriptional variability by selecting isoforms or genes if their FPKM values were >0.01 using the threshold value obtained in the saturation gene coverage analysis [23].

qRT-PCR analysis

The top fully expanded leaves from each plant after 20 d LL-Salt stress treatment were collected for qRT-PCR analysis. Isolated total mRNA with TRIzol Reagent (Invitrogen) was followed by treatment with DNase I (Takara) to remove the genomic DNA. The isolated RNA was reverse transcribed into cDNA using SuperScript VILO cDNA Synthesis Kit (Invitrogen Life Technologies). SYBR Green PCR Master Mix from Applied Biosystems, USA, 4,309,155, was used on a Real-Time PCR System ABI StepOnePlus Applied Biosystems, USA for qRT-PCR. Primers for qRT-PCR were designed using Primer Prime Plus 5 Software version 3.0 (Applied Biosystems, USA) by taking *Actin1* as an internal control reference. The gene's relative expression was quantified compared to *Actin1* through the $2^{-\Delta\Delta\text{CT}}$ method where $\Delta\Delta\text{CT} = \text{CT}$ of the gene of interest^{-CT} [24]. This quantification was done through three biological replicates. The primers used for specific amplifications are summarized in Table S1.

Metabolism analysis

LC-MS/MS (Q Exactive, Thermo Scientific) was employed for non-targeted metabolomics of the leaves of sheepgrass treated with combined LL-Salt. Samples of sheepgrass leaves were collected in a 2 ml Eppendorf tube containing pre-cooled metal beads and immediately kept in liquid nitrogen. The samples were first subjected to a ball mill at 30 Hz for 5 min; the extract powder was dissolved with a mixture of 1.5 ml methanol/chloroform and left for 5 h at -20°C . The mixture was then subjected to centrifugation at a velocity of 2,000g and 4°C for 10 min, and the result was then filtered using the medium of organic phase (GE Healthcare, 6789–0404) of porosity 0.43 μm . The column was 100 \times 2 mm Phenomenex Luna 3 μm NH₂ (Catalog no. 00D-4377-B0, 0.314 mL volume). The injection volume was 20 μL , and the column temperature was at 20°C with a flow speed of 0.4 mL/min. Eluent A: 10 mM Ammonium acetate and 5% (v/v) acetonitrile solution, adjusted to pH 9.5 with ammonia water. Eluent B: acetonitrile. Gradient for elution: 0–1 min, 15% A; 1–8 min, 15–70% A; 8–20 min, 70–95% A; 20–22 min,

95% A; 22–25 min, 15% A. Metabolomic analysis was performed using metabolon software (Durham, NC, USA). All mass spectra of compounds that exist in each sample are identified using metabolic compounds entry of NIST02, as well as entries that exist in the Golm metabolome database entries (<http://csbdb.mpimp-golm.mpg.de/csbdb/gmd/gmd.html>).

Statistical analyses

Two-way ANOVA was performed to determine the possible interaction between the two factors [light (ML or LL) and salt stress (0mM, 50mM, and 200mM)]. Duncan's test was used as a post hoc test for the multiple comparisons between the variants using SPSS 16.0 (SPSS Inc., Chicago, IL, United States). Principal component analysis (PCA) was conducted using singular value decomposition. Heatmaps with dendrograms were produced.

Results

Photosynthetic-physiological response to LL-Salt

Results suggested that the growth of sheepgrass seedlings was phenotypically inhibited either under LL (LL_0 vs. ML_0) or high salt treatment (ML_200 vs. ML_0) (Fig. 1A). In particular, the plants exhibit a more severe lodging phenotype when exposed to LL-Salt combined conditions than under other conditions (Fig. 1A). Consistent with this, F_v/F_m , representing an indicator of photosynthetic capacity, shows at least an 8% reduction ($P < 0.05$) under LL across three NaCl concentrations compared to that under ML condition (ML_0) (Fig. 1B). Salt induces an about 15% reduction in F_v/F_m even under 50mM NaCl, suggesting the NaCl treatments for 20 days are sufficient to inhibit sheepgrass growth. In addition, total sugar content, H_2O_2 , and proline contents were all increased ranging from 6 to 23% under salt stress irrespective of light treatment, except for H_2O_2 under ML_0 condition (Fig. 1C-E). This evidence suggests two different responses for the antioxidant reaction between ML

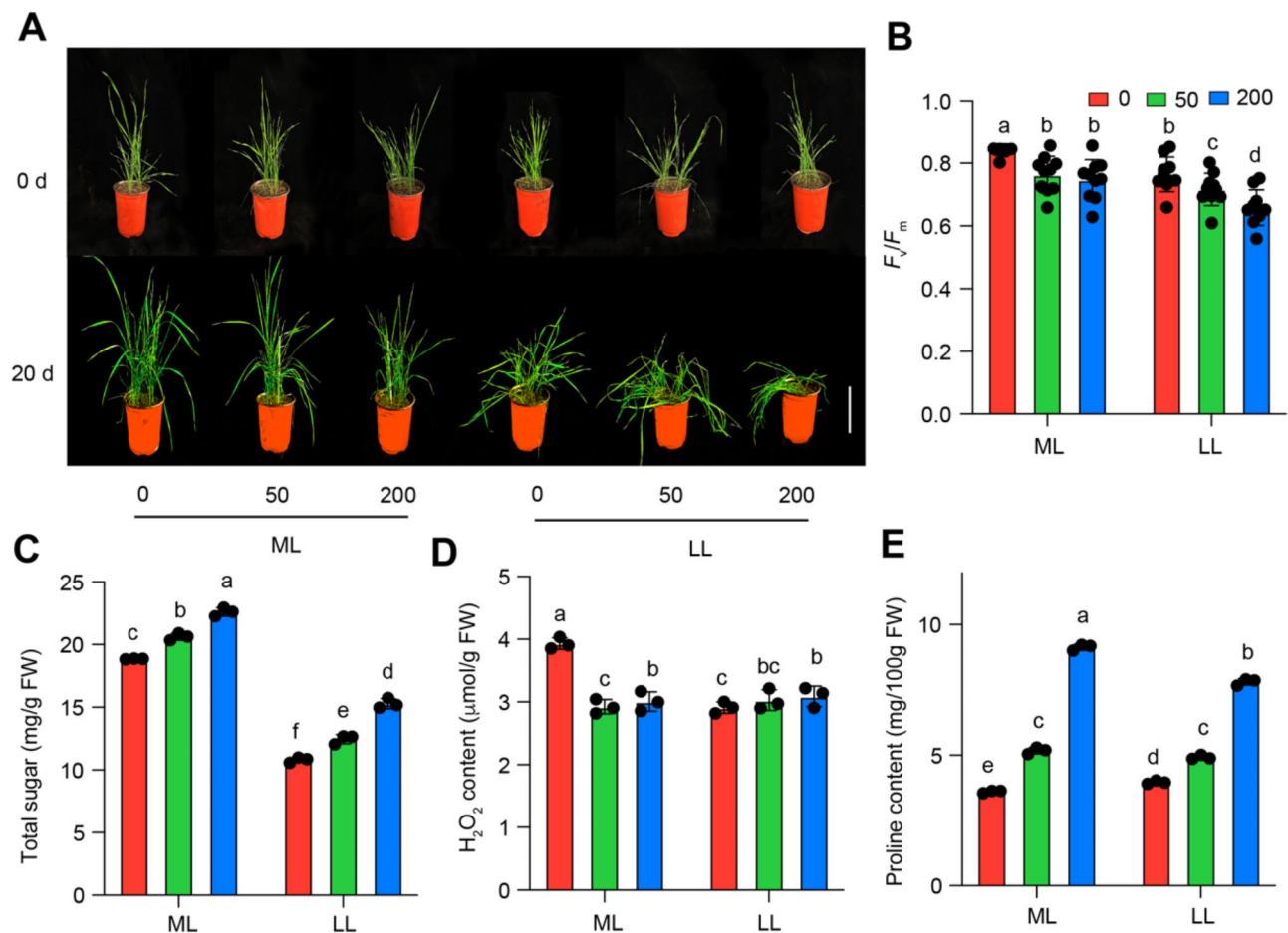


Fig. 1 Performance of sheepgrass seedlings exposed to LL-Salt condition. **A**, Images of sheepgrass plants exposed to LL-Salt condition for 0 and 20 days. The vertical bar represents 5 cm. **B-E**, F_v/F_m , total sugar content, H_2O_2 content, and proline content. Each bar data represents the mean of replicates ($n = 10$ for panel **B** and $n = 4$ for panels **C-E**). Different letters represent significant differences based on one-way ANOVA followed by Tukey's HSD tests ($P < 0.01$)

and LL, although proline contents consistently increased following increased NaCl.

Enzymatic ROS scavenging system in response to LL-Salt stress

To further examine the differences in antioxidant reaction between two light conditions, we measured the activities of SOD, CAT, and MDA. Results suggested that the activities of CAT and POD were significantly decreased by at least 12% following increased NaCl treatment, while they are opposite for MDA and SOD activity (Figure S1A-D). In terms of light treatment with a comparison of ML_0 vs. LL_0, there were different changes in the activities of four antioxidant enzymes, with an increase in CAT and SOD, a decrease in POD, and no significant difference in MDA (Figure S1A-D).

Transcriptome analysis on Sheepgrass leaves exposed to LL-Salt

We performed a transcriptome analysis to identify the key genes with dramatic differences in sheepgrass leaves induced by LL-Salt treatment. Results suggested that the number of clean reads across 18 samples was 65,764,000, accounting for 99.3% (Table S2). The Q30 values across 18 samples were 0.97 (Table S2). Due to limited genome information for sheepgrass, we performed no-references comparisons by mapping the reads to nine genome databases to increase the accuracy of the mapping approach. Results showed that most reads were fine-mapped to the sequence from the Nr database with 21.6% mapping rates, followed by Pfam, Swiss-prot, and gene-ontology blast (Figure S2A). Similarities analysis suggested that samples within the group for each treatment showed a high correlation coefficient with $r > 0.87$. Consistent with this, principal component analysis indicated that the samples exposed to three NaCl treatments were clearly separated, and this is also true for the samples exposed to the two light treatments (Fig. 2A; Figure S2B). The $\log_2(\text{FPKM})$ values across the 18 samples were all around 2, and the distribution of the FPKM values yielded normal distribution (Figure S2C-D). These results confirmed the good quality of the samples used for transcriptome analysis.

LL induced the changes of differentially expressed genes

In this regard, we identified 43,562 genes across the 18 samples (Fig. 2B), and most of the genes were annotated to signal transduction mechanism, post-translational modification, protein turnover, and chaperones except for functional unknown due to limited gene information (Fig. 2C). In addition, very few genes were annotated to extracellular and nuclear structure (Fig. 2C). We then compared the LL-induced changes in global gene expression between the ML_0 vs. LL_0 group. There are 4921

downregulated and 4552 upregulated genes with significant differences (DEGs)(Fig. 3B). The top 1% of DEGs are listed in Table S3. GO and KEGG analysis on the 4,921 downregulated DEGs suggested that the cellular function terms of plastid, plastid part, membrane part, and thylakoid part were significantly enriched in GO analysis. The pathways of starch and sucrose metabolism, photosynthesis, glyoxylate, dicarboxylate metabolism, and carbon metabolism were significantly enriched in the list of KEGG analyses (Fig. 3D). Regarding upregulated DEGs, we found that protein-containing complex, non-membrane-bounded organelle, and intracellular organelle lumen were enriched considerably based on GO analysis (Figure S3A). In contrast, the pathways of the ribosome, valine, leucine, and isoleucine biosynthesis, peroxisome were significantly enriched based on KEGG analysis (Figure S3B).

Salt stress induced the changes of differentially expressed genes

Next, we analyzed the DEGs induced by two salt conditions (50 and 200 mM NaCl). Results suggested that 2,210 DEGs were overlapped between the comparisons of ML_200 vs. ML_0 and ML_40 vs. ML_0 (Fig. 4A). In the overlapped 2,210 DEGs, we found 924 upregulated and 1,286 downregulated DEGs in comparison of ML_200 vs. ML_0, while 875 upregulated and 1,335 downregulated DEGs in comparison of ML_50 vs. ML_0 (Fig. 4B). Furthermore, we identified 301 common upregulated DEGs and 194 common downregulated DEGs in salt-induced comparisons (ML_200 vs. ML_0 and ML_50 vs. ML_0) for the following GO and KEGG analysis (Table S4). GO and KEGG analysis on downregulated DEGs suggested that the pathways of protein phosphorylation, photosynthesis, and phosphate metabolic process were significantly enriched based on GO analysis.

In contrast, starch and sucrose metabolism, pentose phosphate pathways, glyoxylate and dicarboxylate metabolism, and carbon metabolism were enriched considerably based on KEGG analysis (Fig. 4C-D). Regarding upregulated DEGs induced by salt treatment, we found that the pathways of response to stimulus, response to stress, response to external stimulus, and defense response were significantly enriched based on GO analysis. In contrast, based on KEGG analysis, starch and sucrose, glutathione metabolism, arginine and proline interaction, and galactose metabolism were significantly enriched in the upregulated DEGs (Figures S4A-B).

Interactive effects of salt and light on DEGs

We then analyzed the DEGs induced by salt and light interaction effects. Results suggested that 16 overlapped DEGs were identified in both light (including ML_0 vs. LL_0) and salt (both ML_200 vs. ML_0 and

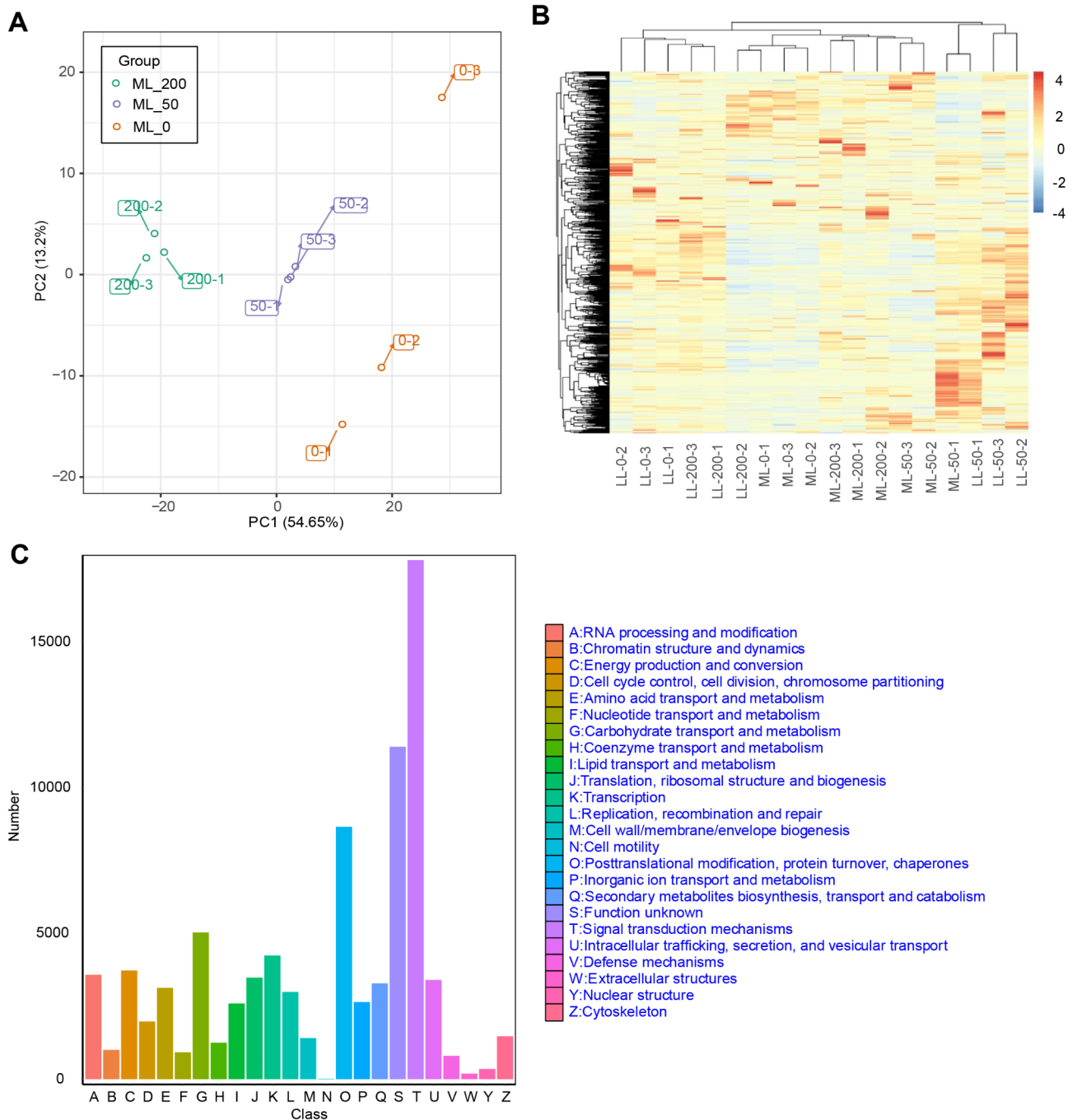


Fig. 2 Transcriptome analysis on the grass exposed to either LL or high salt treatment. **A**, Principal component analysis on the global gene expression of sheepgrass leaves exposed to three salt treatments under ML. **B**, Heatmap representing the relative abundance of the global gene in 18 samples. **C**, Annotated information of biological pathways of the global gene

ML_50 vs. ML_0) groups (Fig. 5A). We named these as LL-Salt responsive genes listed with their relative transcript abundance in Fig. 5B. Furthermore, the six genes with different expression patterns in comparisons of ML_200 vs. ML_0, ML_50 vs. ML_0, and LL_0 vs. ML_0 were selected to conduct qPCR. The results confirmed that the expression levels of a phytochrome-interacting

transcription factor 4 (PIF4) and a WD repeat-containing protein 44 (*WDRCP44*) were increased by LL. In contrast, receptor kinase-like protein Xa21 (*Xa21*), peroxidase 5 (*POD5*), and receptor protein kinase (*ZmPK1* like) were decreased with no significant changes in ABC-transporter genes (Fig. 5B-G). Regarding salt stress, results confirmed that the expression level of *PIF4*, *Xa21*,

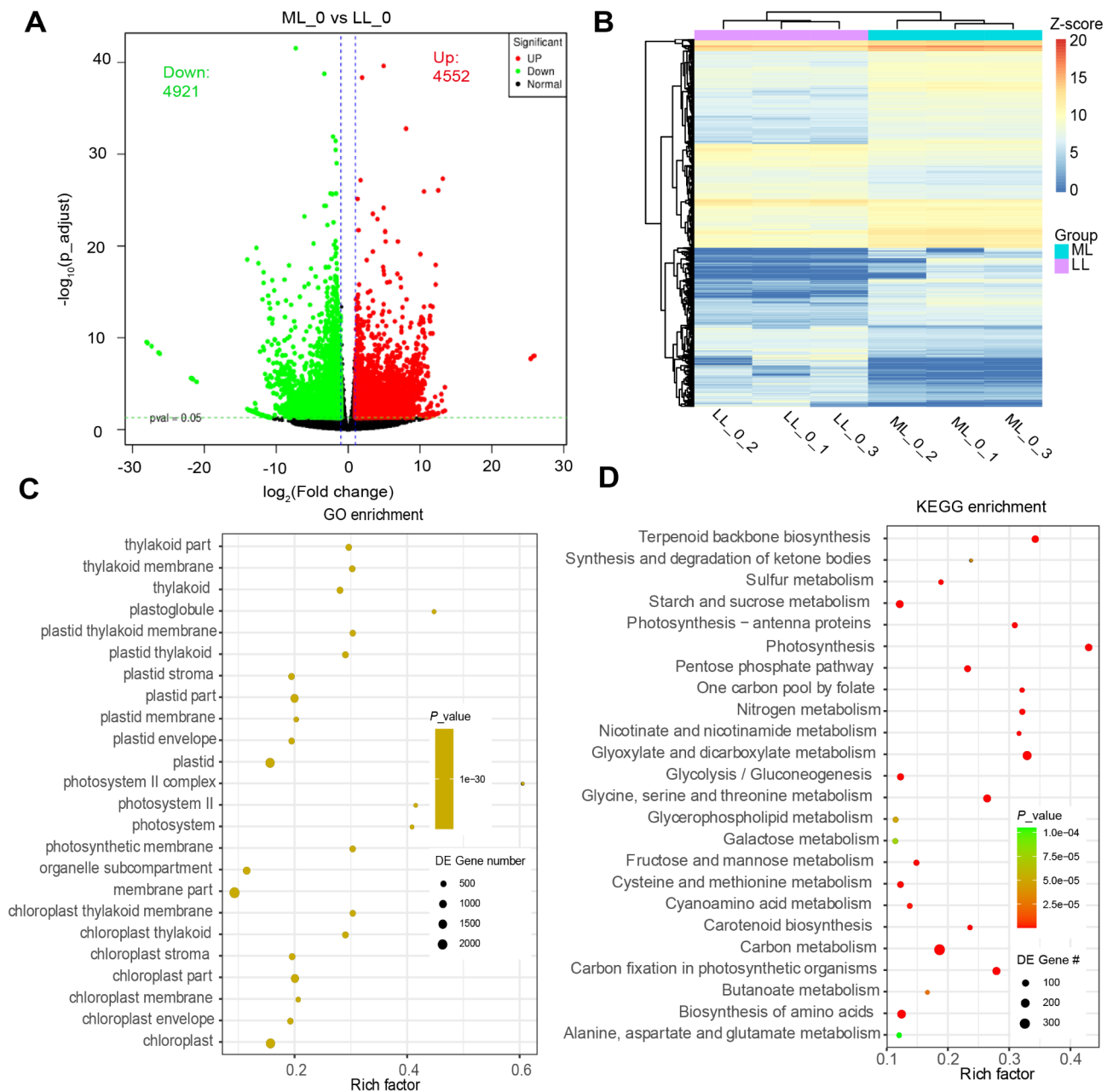


Fig. 3 Low light-induced global expression changes in the grass. **A**, Volcano plot represents the differentially expressed genes compared to ML_0 and LL_0. **B**, heatmap showing the relative abundances of transcripts in six sheepgrass samples exposed to either LL or ML. **C-D**, GO (**C**), and KEGG (**D**) analysis on the list of downregulated DEGs in LL_0 compared it to ML_0

POD5, *ABC-transporter*, and *ZmPK1-like* was decreased, while *WDRCP44* was increased by salt stress (Fig. 5C-G).

Metabolism analysis on Sheepgrass leaves exposed to LL-Salt

Furthermore, we performed a non-targeted metabolism analysis to identify the DAMs in the six combinations of light and salt stress in sheepgrass. Similarities analysis suggested that samples within the group for each treatment showed a high correlation coefficient with $r > 0.92$.

PCA indicated consistently that the samples exposed to three NaCl treatments were clustered together, which is also true for the samples exposed to two light treatments (Fig. 6A; Figure S5A). Most metabolites were identified to annotate in fatty acids, organ-oxygen compounds, carboxylic acids, and derivatives (Figure S5B). The volcano plot showed 65 upregulated DAMs and 56 downregulated DAMs compared to ML_200 vs. ML_0 (Fig. 6B; Table S6).

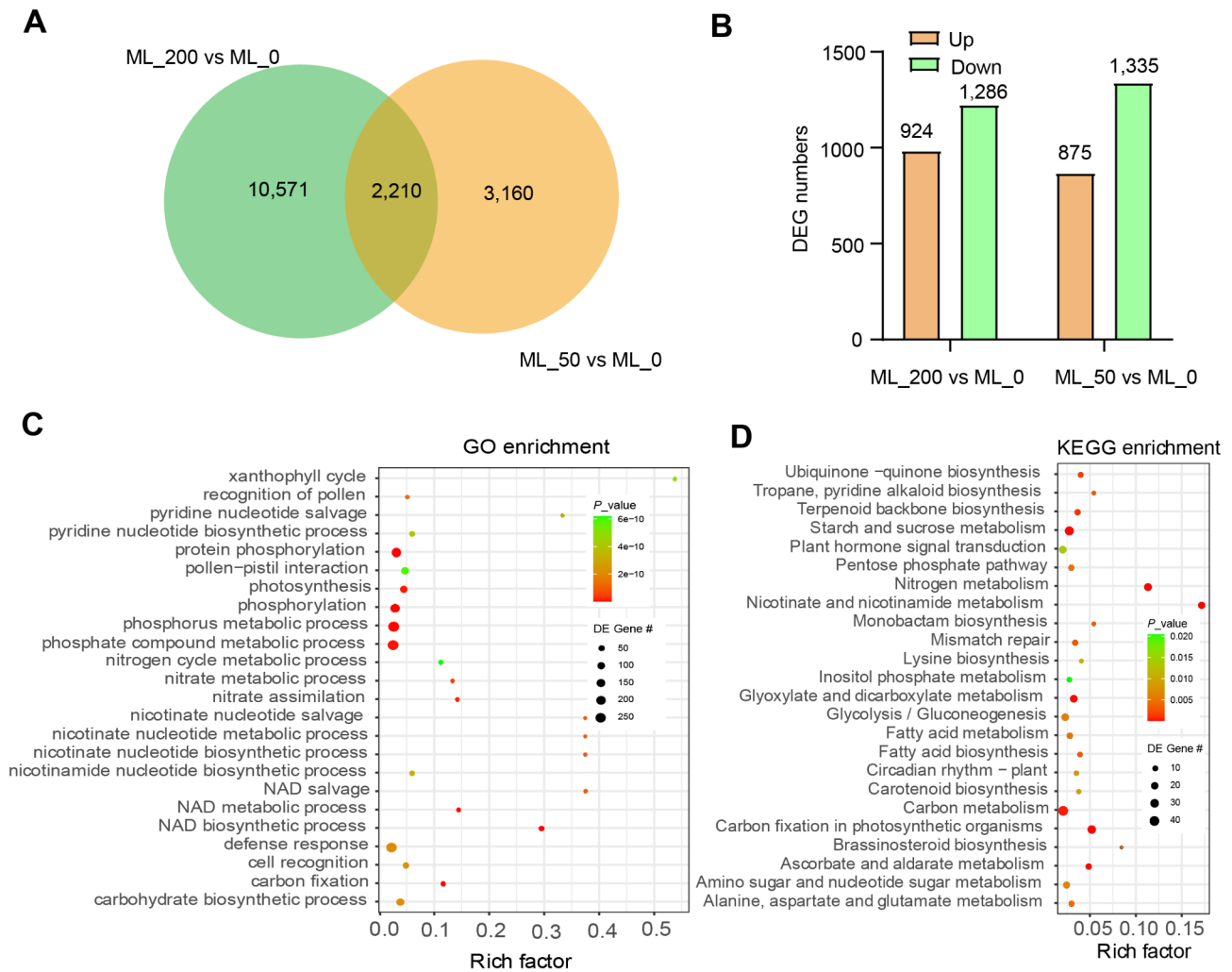


Fig. 4 Salt-induced global gene expression changes in sheepgrass. **A** Venn diagram shows the common differentially expressed genes in comparing two salt treatments (ML_200 vs. ML_0 and ML_50 vs. ML_0). **B** Summary of differentially expressed genes with either upregulated or downregulated patterns in comparing two salt treatments. **C-D**, GO (**C**), and KEGG (**D**) analysis on the list of downregulated DEGs in both salt treatments (ML_200 and ML_50) relative to ML_0

Salt stress-induced DAMs were then analyzed. Venn diagram showed 73 overlapped DAMs between the comparisons of ML_200 vs. ML_0 and ML_50 vs. ML_0 (Fig. 6C; Table S7). KEGG analysis on the list of 278 DAMs in comparison of ML_200 vs. ML_0 suggested that metabolic pathways of GABAergic synapse, protein digestion and absorption, citrate cycle (TCA) cycle, ABC transporter, pyruvate metabolism, glyoxylate, and dicarboxylate metabolism were significantly enriched (Fig. 6D). Furthermore, KEGG analysis on the 35 overlapped DAMs showed the pathways of phenylalanine metabolism, glycine, serine and threonine metabolism, galactose metabolism, and ABC transporter were significantly enriched (Fig. 6E).

In addition, we identified 16 common DAMs between the comparisons of light response (ML_0 vs. LL_0) and salt response (ML_200 vs. ML_0 & ML_50 vs.

ML_0) (Fig. 7A-B; Table S8). Among them, three identified metabolites involved in the TCA cycle were all increased in LL treatment compared to ML, while they were decreased in two salt stress treatments (ML_200 and ML_50) relative to ML_0 (Fig. 7B; Table S8). For the carbon metabolism pathway, we identified that 7 DAMs, including glucose, raffinose, sucrose, D-ribose, D-fructose, D-mannose, and ribulose 5-phosphate, were all downregulated in both light treatment (ML_0 vs. LL_0) and salt treatments (ML_200 vs. ML_0 & ML_50 vs. ML_0). In addition, an identified metabolite, glutathione disulfide, in the GSH/GSSG redox system together with two photorespiratory pathway intermediates, i.e., serine and glycolate, were all downregulated in LL treatment (ML_0 vs. LL_0), while upregulated in the two salt treatments (ML_200 vs. ML_0 & ML_50 vs. ML_0) (Fig. 7B; Table S8).

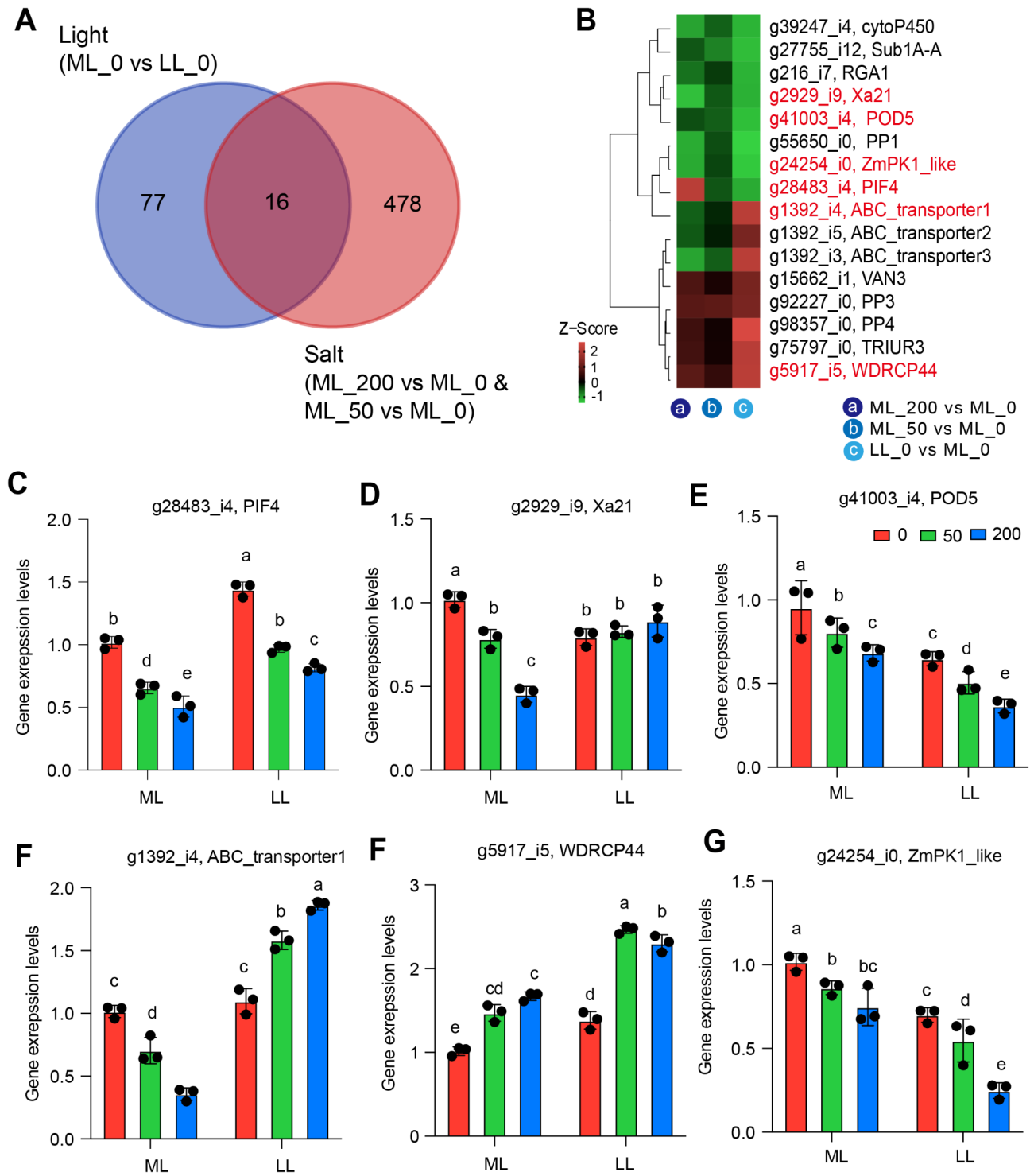


Fig. 5 Interactive effects of salt and light on global gene expression in sheepgrass based on transcriptome analysis. **A**, Venn diagram showing the overlapped genes in comparisons of light (ML_0 vs. LL_0) and two salt treatments (ML_200 vs. ML_0 and ML_50 vs. ML_0). **B**, The relative abundance of the overlapped 18 genes. **C-G**, Relative expression levels of genes involved in the overlapped gene list in sheepgrass leaves exposed to light or salt treatment. Each bar data represents the mean of replicates ($n = 3$). Different letters represent significant differences based on one-way ANOVA followed by Tukey's HSD tests ($P < 0.05$)

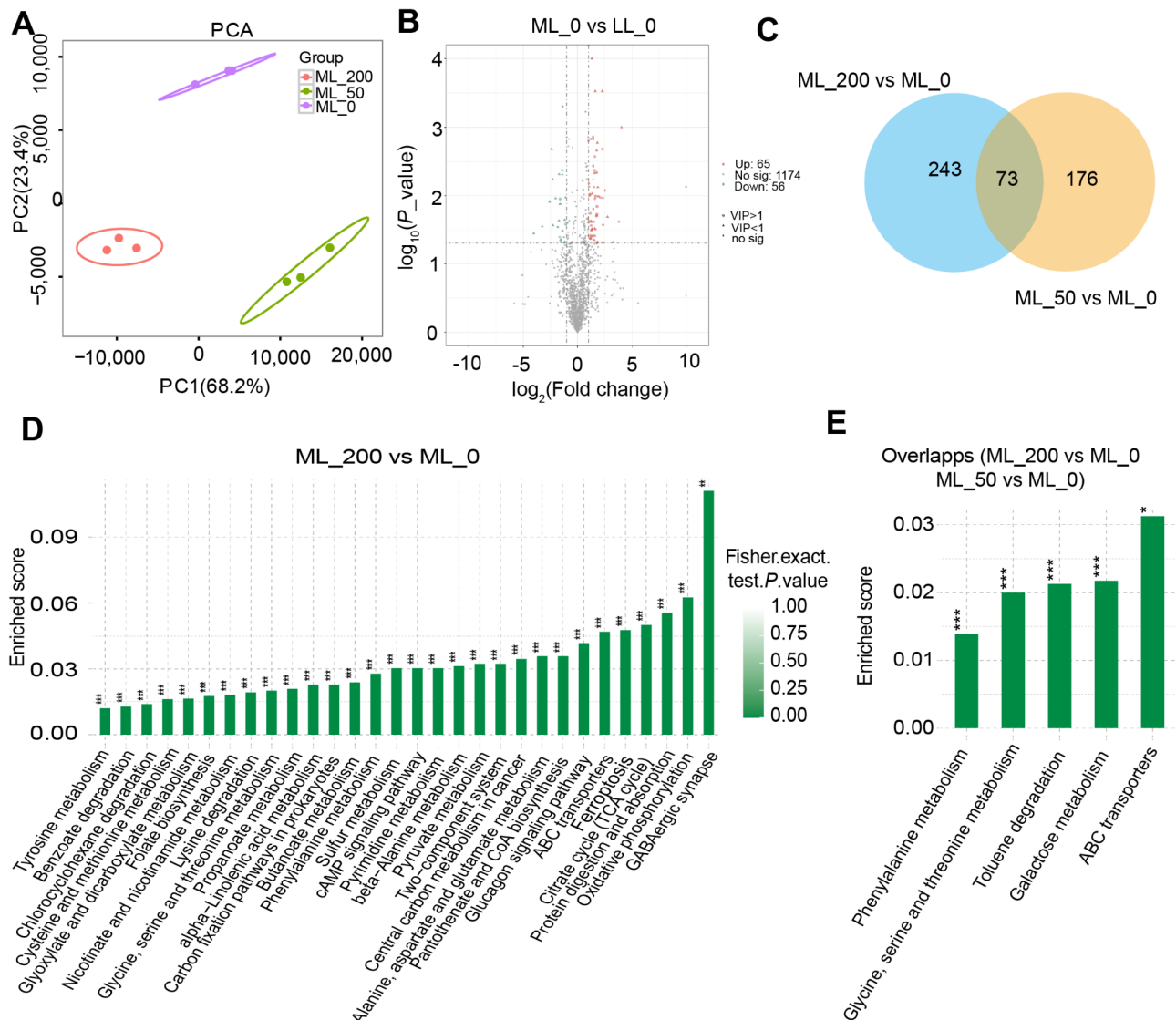


Fig. 6 Differentially abundant metabolites in sheepgrass exposed to either salt or light conditions. **A**, Principal component analysis on the 1,254 identified metabolites of sheepgrass leaves exposed to three salt treatments under ML. **B**, Volcano plot represents the differentially abundant metabolites compared to ML_0 vs. LL_0. **C**, Venn diagram showing the overlapped differentially abundant metabolites in two salt treatments (ML_200 vs. ML_0 and ML_50 vs. ML_0). **D-E**, KEGG analysis on the list of differentially abundant metabolites compared to ML_200 vs. ML_0 and two salt treatments (ML_200 vs. ML_0 and ML_50 vs. ML_0)

qPCR validation on expression of key genes in antioxidant redox pathways

We determined the expression levels of some regulatory genes to validate the patterns of metabolites involved in these metabolic pathways. Results showed that the expression levels of serine/threonine-protein phosphatase 2 (*SuRK2*) in the ABA signaling pathway were significantly increased in both LL treatment and two salt treatments (Fig. 7C; Table S3). The glycolate oxidase gene (*GO1*) expression levels in the photorespiration pathway were decreased significantly by LL treatments but increased dramatically in two salt treatments (Fig. 7D; Table S3). In the GSH/GSSG system, we found that

glutathione reductase (*GRI*) expression levels were significantly decreased by LL treatment but increased considerably by two salt treatments (Fig. 7E; Table S3). The expression levels of three genes were in line with the metabolite's patterns (Fig. 7C-E).

In summary, metabolites involved in carbon metabolism pathways were downregulated, while ABA signaling was upregulated for both LL and salt treatments. Metabolites involved in the photorespiration pathway and GSH/GSSG redox system were downregulated and upregulated; reversely, the TCA cycle was upregulated and downregulated in LL and salt treatment, respectively (Fig. 7F). Accordingly, the activities of some enzymes

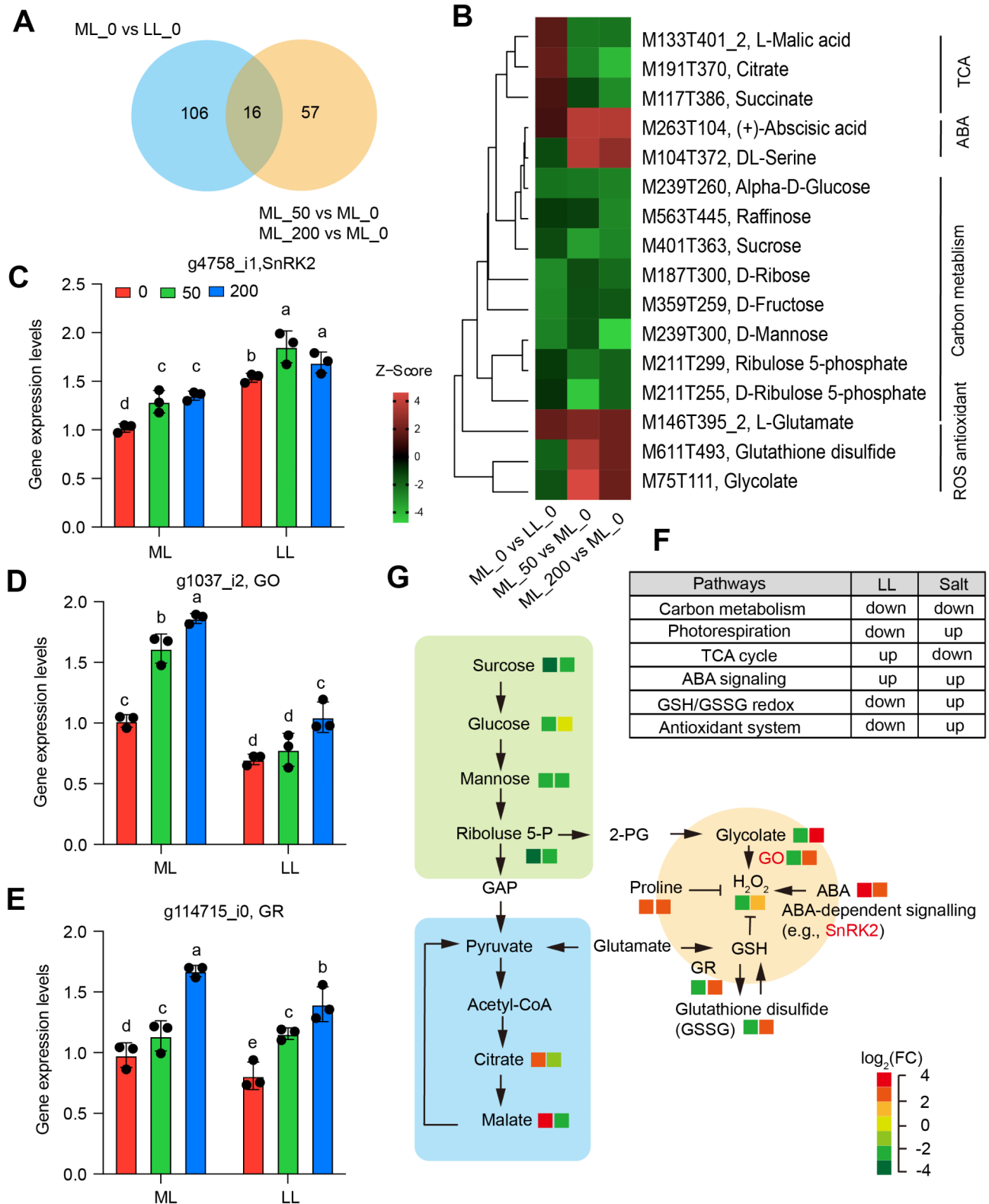


Fig. 7 Summary of the key metabolic pathways in low light and salt stress response in sheepgrass. **A**, Venn diagram of differentially abundant metabolites in comparisons of salt and light treatments. **B**, Heatmap representing the relative abundance of overlapped differentially abundant metabolites in comparisons of light (ML₀ vs. LL₀) and salt (ML₂₀₀ vs. ML₀ & ML₅₀ vs. ML₀). **C-E**, Relative expression levels of genes involved in ABA signaling pathway, photorespiration, and GSH/GSSG redox system pathways in sheepgrass leaves exposed to either LL or salt treatments. **F**, Summary of regulation pattern of key metabolic pathways in response to low light and salt stress in sheepgrass leaves. **G**, Working model showing the interactive effects of LL and salt on key metabolic pathways in sheepgrass leaves

involved in the antioxidant system, including CAT, were downregulated and upregulated by LL and salt treatment, respectively (Figure S1A; Fig. 7F). Finally, we summarized LL and salt's reprogrammed primary metabolic pathways (Fig. 7G). Both LL and salt inhibited the pentose phosphate pathway; in particular, sucrose contents declined in both LL and salt treatments. Salt stimulates photorespiration, leading to the accumulation of H_2O_2 , together with ABA signaling, proline, and GSSG accumulation (Fig. 7G). In contrast, LL inhibits photorespiration, hence resulting in less production in H_2O_2 , collectively working with GSSG reduction (Fig. 7G). Therefore, LL and salt function in ROS production in different directions, suggesting essential roles of redox homeostasis in LL-Salt combined treatments.

Discussions

LL always occurs in natural conditions due to, but not limited to, cloud cover and canopy shading, which affects the growth of plants from gene expression and metabolites to morphological regulations [11–13]. In particular, LL and other adverse stressors, such as salinity, intensify growth inhibition by reprogramming these biological processes [15, 25]. Sheepgrass is a promising model material for studying salt tolerance [2]. However, the mechanism of how biological pathways respond to such an LL-salt combined process has not yet been explored. In this study, through combined analysis of transcriptome and metabolism, we demonstrated that several metabolic pathways were essential for adaptation to LL-Salt in sheepgrass. LL and salt treatments induce downregulation of carbon metabolism and upregulation of the ABA signaling pathway. Interestingly, the two stresses also have separate regulatory pathways, and they primarily function differently in cellular redox homeostasis.

Downregulation of sucrose metabolism in LL-Salt combined condition

Sugars are important metabolic resources and structural components of plant cells that can usually undergo osmotic adjustment under various stress conditions, including salt stress [26–29]. Sucrose, as a disaccharide, acts as the central carbon and energy source in the metabolism of plants. The regulation of some combined stressful conditions, including drought and heat stress by plants, initiates an adjustment in sucrose content and promotes carbohydrate redistribution and degradation into glucose for adaptation to such combined stressful conditions [30]. Consistent with the study's observation, our finding shows that LL-Salt combined stress causes a dramatic reduction in sucrose and other metabolites in the carbon metabolic pathway, including fructose, mannose, and ribose. This evidence suggested that sucrose was hydrolyzed into small molecular carbohydrates

adjusted to different cases of combined stressful conditions. The sucrose metabolic pathway is tightly linked to photosynthetic carbon metabolism, exacerbating the decline in photosynthetic carbon assimilation under such combined conditions [31], as indicated by the reduction in photosynthetic efficiency, including F_v/F_m , which inhibit energy-containing substances such as ATP [32], with photorespiration reduction [33].

Photorespiration downregulated by LL but upregulated by salt stress

A bypass pathway of carbon metabolism in which photorespiration has emerged as a subsidiary participant for the photosynthetic assimilation of CO_2 and ROS generation [34]. The growth LL intensity greatly influences the evolution of the photorespiratory pathway [35]. While intermediates in photorespiration like glycolate and glycerate are inhibitors of the Calvin cycle [34], the photorespiratory pathway converts them into glycerate-3-phosphate [36]. In photosynthesis and photoprotection, such a process is essential [37]. Hence, it postulates its possible dual role within carbon assimilation metabolism. Interestingly, salt stress may promote photorespiration, the opposite of what occurred under LL (Fig. 7F-G), possibly because it has a vital role in inhibiting the accumulation of free radicals (ROS) to maintain cellular redox homeostasis [38].

Oxidative damage repair and defense response under salt stress

Oxidative stress, caused by an over-accumulation of ROS, is directly associated with cell damage related to salt stress [39]. We measured the activities of SOD, POD, MDA, and CAT to find out whether antioxidant enzymes can enhance ROS scavenging and alleviate oxidative damage under LL-Salt combined stress in the leaves of sheepgrass. In general, POD, SOD, MDA, and CAT are plant-specific enzymes of the process of lignin formation, cross-linking components of the cell wall, and removal of H_2O_2 against abiotic stresses [40, 41]. Our results show that activities of CAT and POD are decreased due to salt stress but showed an opposite pattern in response to LL, while activities of MDA and SOD were increased by salt, and two enzymes showed similar or increase in LL response (Figure S1A-B). The result suggests that the antioxidant serves other functions depending on the salinity concentration and LL. However, under whatever conditions, H_2O_2 removal must occur whenever plants experience a combination of LL-salt stress in the sheepgrass leaf. This could serve as part of the adaptation by plants under such stress [42, 43]. On the other hand, several research experiments demonstrated that, at least during the early stages, both LL and salt stress-induced

ROS accumulation may act as a protective process rather than a harmful one [41, 44, 45].

Based on our transcriptome analysis, we found that several genes involved in the ROS signaling pathway were downregulated and upregulated by LL and salt stress, respectively, e.g., *GOI* (glycolate oxidase 1, g1037_i2) and *GRI* (glutathione reductase 1, g114715_i0) (Fig. 7D-E; Table S3). *GRI* is responsible for maintaining the supply of reduced glutathione (M611T493) (Fig. 7B) for cellular control of ROS [46]. At the same time, *GOI* catalyzes glycolate (M75T111)(Fig. 7B), acting as a significant engine for H₂O₂ production [47]. The expression changes of two genes (*GRI* and *GOI*) aligned with H₂O₂ changes in response to LL-Salt treatments.

Roles of GSH/GSSH redox system in removal of ROS under LL-Salt

The ascorbate-glutathione cycle constitutes part of the redox system that adjusts growth and development to changing environmental conditions, such as light intensity variations and light spectrum [48–50]. Notably, glutathione reductases, or GR, catalyze GSSG back into GSH, an activity important in detoxifying the H₂O₂ molecules as part of the ascorbate-glutathione cycle. Along with that reduction of light intensity, its reduced (GSH) and the oxidized form (GSSG) and its GSSG/GSH ratio also declined. It is further stated that the crops of the crop, which also comprises soybean, possess a much lower GR activity and an amount of GSH in the shaded shade compared to that of full sunlight [51, 52]. Knowing this, our results show that the glutathione reductase expression levels were also reduced significantly in the leaves of sheepgrass subjected to LL treatments, which led to higher GSSG levels than that under ML.

Effects of LL-salt combined stress on TCA cycle

The citrate cycle is one of the most important metabolic pathways, and it provides significant energy resources, such as ATP and NADPH, for growth development [53]. It is first converted from mitochondria to chloroplast as pyruvate, which converts to acetyl-CoA and initiates TCA by producing many amino acids such as citrate, succinate, and malate. More precisely, malate and citrate form the basis of the characteristic flexibility of central plant metabolism by linking mitochondrial respiratory metabolism [54]. Our metabolism analyses showed that all three metabolites were upregulated in LL condition but downregulated in salt stress (Fig. 7B). The reduction in the three metabolites under salt stress suggests oxidative stress occurs, as observed in another study in barley [55]. In addition, the TCA cycle is active in the light at the same rate as in the dark except for a transitory initial inhibition at the onset of light after dark [56], indicating higher impacts of salt stress than that under LL

conditions. Our results showed that TCA played a crucial role in salt responses since this would change the content of specific metabolites because of other related species before [57].

Conclusions

This study revealed that the growth and photosynthetic capacity of sheepgrass seedlings was dramatically inhibited by LL-Salt combined treatments. Through integrated analysis of transcriptome and metabolism, we found that carbon metabolism pathways were significantly enriched in the differentially expressed genes with downregulation by both LL and salt stress treatment. Several antioxidant redox pathways, including photorespiration, GSG/GSSH redox, and ABA signaling, participated in response to LL and salt combined events and highlighted the roles of cellular redox homeostasis in LL-Salt response in sheepgrass. This study provides insight into how plants mediate cellular redox homeostasis to maintain growth development in such LL-Salt combined events in sheepgrass, which could help to guide precise molecular assistant selection in sheepgrass.

Supplementary Information

The online version contains supplementary material available at <https://doi.org/10.1186/s12864-025-11526-9>.

Supplementary Material 1

Supplementary Material 2

Acknowledgements

Not applicable.

Author contributions

MQ and JL planned and designed the research. JL, SF, HZ, ZI, CS, WH, KH, XM, MD, ZL and BG performed experiments. JL, SF and HZ analysed data. JL, MQ and ZI wrote the manuscript.

Funding

This work was supported by the Heilongjiang Agricultural Science and Technology Innovation Cross Engineering, Agricultural Science and Technology Basic Innovation Project (CX22JQ04), and the National Natural Science Foundation of China (32170245).

Data availability

The related RNA sequencing datasets used in the current study are deposited in NCBI GEO database, <https://www.ncbi.nlm.nih.gov/geo/query/acc.cgi?acc=GSE284307>.

Declarations

Ethics approval and consent to participate

Our rice collection work complies with the laws of the People's Republic of China and has a permission letter from the Institute of Grass Research, Heilongjiang Academy of Agricultural Sciences. Voucher specimens were identified by Prof. Wei Li (Heilongjiang Academy of Agricultural Sciences) and kept at Heilongjiang Rice Quality Improvement and Genetic Breeding Engineering Research Center (No: SG001-SG058). All methods were carried out in accordance with relevant guidelines and regulations.

Consent for publication

Not applicable.

Competing interests

The authors declare no competing interests.

Received: 4 December 2024 / Accepted: 25 March 2025

Published online: 29 March 2025

References

- Panigrahy M, Majeed N, Panigrahi KC. Low-light and its effects on crop yield: genetic and genomic implications. *J Biosci.* 2020;45(1):102.
- Li T, Tang S, Li W, Zhang S, Wang J, Pan D, Lin Z, Ma X, Chang Y, Liu B. Genome evolution and initial breeding of the triticeae grass *Leymus chinensis* dominating the Eurasian steppe. *Proc Natl Acad Sci.* 2023;120(44):e2308984120.
- Peng X, Ma X, Fan W, Su M, Cheng L, Iftekhar A, et al. Improved drought and salt tolerance of *Arabidopsis thaliana* by transgenic expression of a novel DREB gene from *Leymus chinensis*. *Plant Cell Rep.* 2011;30:1493–1502.
- Munns R, Tester M. Mechanisms of salinity tolerance. *Annu Rev Plant Biol.* 2008;59(1):651–81.
- Hasanuzzaman M, Nahar K, Anee TI, Fujita M. Glutathione in plants: biosynthesis and physiological role in environmental stress tolerance. *Physiol Mol Biology Plants.* 2017;23:249–68.
- Greenway H, Munns R. Mechanisms of salt tolerance in nonhalophytes. *Annu Rev Plant Physiol.* 1980;31(1):149–90.
- Ji H, Pardo JM, Batelli G, Van Oosten MJ, Bressan RA, Li X. The salt overly sensitive (SOS) pathway: established and emerging roles. *Mol Plant.* 2013;6(2):275–86.
- Zhu J-K. Abiotic stress signaling and responses in plants. *Cell.* 2016;167(2):313–24.
- Li J, Zhou H, Zhang Y, Li Z, Yang Y, Guo Y. The GSK3-like kinase BIN2 is a molecular switch between the salt stress response and growth recovery in *Arabidopsis thaliana*. *Dev Cell.* 2020;55(3):367–80. e366.
- Lou L, Yu F, Tian M, Liu G, Wu Y, Wu Y, Xia R, Pardo JM, Guo Y, Xie Q. ESCR1 component VPS23A sustains salt tolerance by strengthening the SOS module in *Arabidopsis*. *Mol Plant.* 2020;13(8):1134–48.
- Wang M, Wei H, Jeong BR. Lighting direction affects leaf morphology, stomatal characteristics, and physiology of head lettuce (*Lactuca sativa* L.). *Int J Mol Sci.* 2021;22(6):3157.
- Leonel LV, de Oliveira Reis F, de Assis Figueiredo FAMM, Ferraz TM, de Oliveira Maia Júnior S, Silva PC, de Andrade JR. Light intensity and hydrogel soil amendment differentially affect growth and photosynthesis of successional tree species. *J Forestry Res.* 2023;34(1):257–68.
- Cheng X, Wang R, Liu X, Zhou L, Dong M, Rehman M, Fahad S, Liu L, Deng G. Effects of light spectra on morphology, gaseous exchange, and antioxidant capacity of industrial hemp. *Front Plant Sci.* 2022;13:937436.
- Boccaccini A, Legris M, Krahermer J, Allenbach-Petrolati L, Goyal A, Galvan-Ampudia C, Vernoux T, Karayekov E, Casal JJ, Fankhauser C. Low blue light enhances phototropism by releasing cryptochrome1-mediated inhibition of PIF4 expression. *Plant Physiol.* 2020;183(4):1780–93.
- Liu S, Xu Z, Essemine J, Liu Y, Liu C, Zhang F, Iqbal Z, Qu: GWAS unravels acid phosphatase ACP2 as a photosynthesis regulator under phosphate starvation conditions through modulating Serine metabolism in rice. *Plant Commun.* 2024;5(7):100885.
- Shi H, Wang Y, Cheng Z, Ye T, Chan Z. Analysis of natural variation in Bermudagrass (*Cynodon dactylon*) reveals physiological responses underlying drought tolerance. *PLoS ONE.* 2012;7(12):e53422.
- Bates LS, Waldren R, Teare I. Rapid determination of free proline for water-stress studies. *Plant Soil.* 1973;39:205–7.
- Hamdani S, Qu M, Xin C-P, Li M, Chu C, Zhu X-G. Variations between the photosynthetic properties of elite and landrace Chinese rice cultivars revealed by simultaneous measurements of 820 Nm transmission signal and chlorophyll a fluorescence induction. *J Plant Physiol.* 2015;177:128–38.
- Essemine J, Xiao Y, Qu M, Mi H, Zhu X-G. Cyclic electron flow may provide some protection against PSII photoinhibition in rice (*Oryza sativa* L.) leaves under heat stress. *J Plant Physiol.* 2017;211:138–46.
- Jiang C, Bi Y, Mo J, Zhang R, Qu M, Feng S, Essemine J. Proteome and transcriptome reveal the involvement of heat shock proteins and antioxidant system in thermotolerance of clematis Florida. *Sci Rep.* 2020;10(1):8883.
- Dobin A, Davis CA, Schlesinger F, Drenkow J, Zaleski C, Jha S, Batut P, Chaisson M, Gingeras TR. STAR: ultrafast universal RNA-seq aligner. *Bioinformatics.* 2013;29(1):15–21.
- Love MI, Huber W, Anders S. Moderated Estimation of fold change and dispersion for RNA-seq data with DESeq2. *Genome Biol.* 2014;15:1–21.
- Zhou S, He L, Lin W, Su Y, Liu Q, Qu M, Xiao L. Integrative analysis of transcriptome and metabolism reveals potential roles of carbon fixation and photorespiratory metabolism in response to drought in Shanlan upland rice. *BMC Genomics.* 2022;23(1):862.
- Livak KJ, TD Schmittgen 2001 Analysis of relative gene expression data using real-time quantitative PCR and the 2- $\Delta\Delta$ CT method. *Methods* 25 4 402–8.
- Qu M, Zheng G, Hamdani S, Essemine J, Song Q, Wang H, Chu C, Sirault X, Zhu X-G: leaf photosynthetic parameters related to biomass accumulation in a global rice diversity survey. *Plant Physiol.* 2017;175(1):248–58.
- Li J, Essemine J, Bunce JA, Shang C, Zhang H, Sun D, Chen G, Qu M. Roles of heat shock protein and reprogramming of photosynthetic carbon metabolism in thermotolerance under elevated CO₂ in maize. *Environ Exp Bot.* 2019;168:103869.
- Kaplan F, Kopka J, Haskell DW, Zhao W, Schiller KC, Gatzke N, Sung DY, Guy CL. Exploring the temperature-stress metabolome of *Arabidopsis*. *Plant Physiol.* 2004;136(4):4159–68.
- Rosa M, Prado C, Podazza G, Interdonato R, González JA, Hilal M, Prado FE. Soluble sugars: metabolism, sensing and abiotic stress: A complex network in the life of plants. *Plant Signal Behav.* 2009;4(5):388–93.
- Qu M, Essemine J, Li M, Chang S, Chang T, Chen G-Y, Zhu X-G. Genome-wide association study unravels LRK1 as a dark respiration regulator in rice (*Oryza sativa* L.). *Int J Mol Sci.* 2020;21(14):4930.
- Zandalain S, Mittler R, Balfagón D, Arbona V, Gómez-Cadenas A. Plant adaptations to the combination of drought and high temperatures. *Physiol Plant.* 2018;162(1):2–12.
- Antonovsky N, Gleizer S, Milo R. Engineering carbon fixation in *E. coli*: from heterologous RuBisCO expression to the Calvin–Benson–Bassham cycle. *Curr Opin Biotechnol.* 2017;47:83–91.
- Jones P. Central role for ATP in determining some aspects of animal and plant cell behaviour. *J Theor Biol.* 1972;34(1):1–13.
- Keren N, Krieger-Liszka A. Photoinhibition: molecular mechanisms and physiological significance. *Physiol Plant.* 2011;142(1).
- Timm S, Florian A, Arrivault S, Stitt M, Fernie AR, Bauwe H. Glycine decarboxylase controls photosynthesis and plant growth. *FEBS Lett.* 2012;586(20):3692–7.
- Huang W, Zhang S-B, Hu H. Sun leaves up-regulate the photorespiratory pathway to maintain a high rate of CO₂ assimilation in tobacco. *Front Plant Sci.* 2014;5:688.
- Peterhansel C, Maurino VG. Photorespiration redesigned. *Plant Physiol.* 2011;155(1):49–55.
- Takahashi S, Bauwe H, Badger M. Impairment of the photorespiratory pathway accelerates photoinhibition of photosystem II by suppression of repair but not acceleration of damage processes in *Arabidopsis*. *Plant Physiol.* 2007;144(1):487–94.
- Voss I, Sunil B, Scheibe R, Raghavendra A. Emerging concept for the role of photorespiration as an important part of abiotic stress response. *Plant Biol.* 2013;15(4):713–22.
- Lyon BR, Lee PA, Bennett JM, DiTullio GR, Janech MG. Proteomic analysis of a sea-ice diatom: salinity acclimation provides new insight into the Dimethylsulfoniopropionate production pathway. *Plant Physiol.* 2011;157(4):1926–41.
- Zheng L, Meng Y, Ma J, Zhao X, Cheng T, Ji J, Chang E, Meng C, Deng N, Chen L. Transcriptomic analysis reveals importance of ROS and phytohormones in response to short-term salinity stress in *Populus tomentosa*. *Front Plant Sci.* 2015;6:678.
- Miller G, Suzuki N, Ciftci-Yilmaz S, Mittler R. Reactive oxygen species homeostasis and signalling during drought and salinity stresses. *Plant Cell Environ.* 2010;33(4):453–67.
- Xu Z, Zhang J, Wang X, Essemine J, Jin J, Qu M, Xiang Y, Chen W. Cold-induced inhibition of photosynthesis-related genes integrated by a TOP6 complex in rice mesophyll cells. *Nucleic Acids Res.* 2023;51(4):1823–42.
- Zhao Q, Tobimatsu Y, Zhou R, Pattathil S, Gallego-Giraldo L, Fu C, Jackson LA, Hahn MG, Kim H, Chen F. Loss of function of cinnamyl alcohol dehydrogenase 1 leads to unconventional lignin and a temperature-sensitive growth defect in *Medicago truncatula*. *Proceedings of the National Academy of Sciences.* 2013;110(33):13660–13665.

44. Shi Z, Chang T, Chen G, Song Q, Wang Y, Zhou Z, Wang M, Qu M, Wang B, Zhu X. Dissection of mechanisms for high yield in two elite rice cultivars. *Field Crops Res.* 2019;241:107563.
45. Pang C-H, Wang B-S. Oxidative stress and salt tolerance in plants. In: *Progress in botany*. Springer; 2008: 231–245.
46. Couto N, Wood J, Barber J. The role of glutathione reductase and related enzymes on cellular redox homeostasis network. *Free Radic Biol Med.* 2016;95:27–42.
47. Li X, Liao M, Huang J, Xu Z, Lin Z, Ye N, Zhang Z, Peng X. Glycolate oxidase-dependent H₂O₂ production regulates IAA biosynthesis in rice. *BMC Plant Biol.* 2021;21:1–14.
48. Noctor G, Mhamdi A, Chaouch S, Han Y, Neukermans J, Marquez-Garcia B, Queval G, Foyer CH. Glutathione in plants: an integrated overview. *Plant Cell Environ.* 2012;35(2):454–84.
49. Heyneke E, Luschin-Ebengreuth N, Krajczer I, Wolkingner V, Müller M, Zechmann B. Dynamic compartment specific changes in glutathione and ascorbate levels in *Arabidopsis* plants exposed to different light intensities. *BMC Plant Biol.* 2013;13:1–19.
50. Toldi D, Gyugos M, Darkó É, Szalai G, Gulyás Z, Gierczik K, Székely A, Boldizsár Á, Galiba G, Müller M. Light intensity and spectrum affect metabolism of glutathione and amino acids at transcriptional level. *PLoS ONE.* 2019;14(12):e0227271.
51. Bartoli CG, Tambussi EA, Diego F, Foyer CH. Control of ascorbic acid synthesis and accumulation and glutathione by the incident light Red/far red ratio in *Phaseolus vulgaris* leaves. *FEBS Lett.* 2009;583(1):118–22.
52. Shainberg O, Rubin B, Rabinowitch HD, Libal-Weksler Y, Tel-Or E. Adjustment to low light intensity enhances susceptibility of bean leaves to oxidative stress. *J Plant Physiol.* 1999;155(3):393–8.
53. Li J, Cui G, Hu G, Wang M, Zhang P, Qin L, Shang C, Zhang H, Zhu X, Qu M. Proteome dynamics and physiological responses to short-term salt stress in *Leymus chinensis* leaves. *PLoS ONE.* 2017;12(8):e0183615.
54. Lee CP, Elsässer M, Fuchs P, Fenske R, Schwarzländer M, Millar AH. The versatility of plant organic acid metabolism in leaves is underpinned by mitochondrial malate–citrate exchange. *Plant Cell.* 2021;33(12):3700–20.
55. Widodo, Patterson JH, Newbigin E, Tester M, Bacic A, Roessner U. Metabolic responses to salt stress of barley (*Hordeum vulgare* L.) cultivars, Sahara and Clipper, which differ in salinity tolerance. *J Exp Bot.* 2009;60(14):4089–103.
56. Chapman EA, Graham D. The effect of light on the Tricarboxylic acid cycle in green leaves: I. Relative rates of the cycle in the dark and the light. *Plant Physiol.* 1974;53(6):879–85.
57. Piro A, Marín-Guirao L, Serra IA, Spadafora A, Sandoval-Gil JM, Bernardeau-Esteller J, Fernandez JM, Mazzuca S. The modulation of leaf metabolism plays a role in salt tolerance of *Cymodocea nodosa* exposed to hypersaline stress in mesocosms. *Front Plant Sci.* 2015;6:464.

Publisher's note

Springer Nature remains neutral with regard to jurisdictional claims in published maps and institutional affiliations.